Binding of κ-Conotoxin PVIIA to *Shaker* K$^+$ Channels Reveals Different K$^+$ and Rb$^+$ Occupancies within the Ion Channel Pore

Anna Boccaccio,[1] Franco Conti,[2] Baldomero M. Olivera,[3] and Heinrich Terlau[1]

[1]Max-Planck-Institute for Experimental Medicine, Molecular and Cellular Neuropharmacology Group, D-37075 Göttingen, Germany
[2]Istituto di Biofisica, Consiglio Nazionale delle Ricerche, I-16149 Genova, Italy
[3]Department of Biology, University of Utah, Salt Lake City, UT 84112

ABSTRACT The x-ray structure of the KcsA channel at different [K$^+$] and [Rb$^+$] provided insight into how K$^+$ channels might achieve high selectivity and high K$^+$ transit rates and showed marked differences between the occupancies of the two ions within the ion channel pore. In this study, the binding of κ-conotoxin PVIIA (κ-PVIIA) to *Shaker* K$^+$ channel in the presence of K$^+$ and Rb$^+$ was investigated. It is demonstrated that the complex results obtained were largely rationalized by differences in selectivity filter occupancy of this 6TM channels as predicted from the structural work on KcsA. κ-PVIIA inhibition of the *Shaker* K$^+$ channel differs in the closed and open state. When K$^+$ is the only permeant ion, increasing extracellular [K$^+$] decreases κ-PVIIA affinity for closed channels by decreasing the "on" binding rate, but has no effect on the block of open channels, which is influenced only by the intracellular [K$^+$]. In contrast, extracellular [Rb$^+$] affects both closed- and open-channel binding. As extracellular [Rb$^+$] increases, (a) binding to the closed channel is slightly destabilized and acquires faster kinetics, and (b) open channel block is also destabilized and the lowest block seems to occur when the pore is likely filled only by Rb$^+$. These results suggest that the nature of the permeant ions determines both the occupancy and the location of the pore site from which they interact with κ-PVIIA binding. Thus, our results suggest that the permeant ion(s) within a channel pore can determine its functional and pharmacological properties.

KEY WORDS: voltage-gated potassium channels • permeation • conotoxins • pore block • *Xenopus* oocytes

INTRODUCTION

Potassium channels are highly selective for K$^+$; the x-ray analysis of MacKinnon and coworkers provided the first structure at atomic resolution for any K$^+$ channel (Doyle et al., 1998). They analyzed KcsA, a K$^+$ channel from *Streptomyces lividans*, and found multiple ion occupancy of the pore, which was predicted by electrophysiological experiments (Hodgkin and Keynes, 1955; Armstrong, 1971; Hille and Schwarz, 1978). Five binding sites for K$^+$ along the pore axis were defined; four are in a narrow, 12-Å-long segment adjacent to the extracellular pore opening, and these are numbered starting from the outer side of the selectivity filter. The fifth is in a large water-filled cavity, ∼10 Å in diameter, at the center of the pore near the cytoplasmic end of the selectivity filter. In addition, two ion peaks were observed just beyond the external end of the pore, and these were interpreted to be alternative positions of a single K$^+$ ion at the extracellular side of the pore.

The K$^+$ binding sites cannot be occupied simultaneously, and at high concentrations of K$^+$, there appear to be two isoenergetic configurations of maximal occupancy: the K$^+$ ions either occupy the first, third, and fifth (cavity) sites, or the second and fourth sites and the extracellular site. During permeation, the ions in the pore shift their positions, and with the entrance of a "new" ion either from the extracellular or intracellular side, the last ion at the opposite end of the pore exits (Morais-Cabral et al., 2001; Zhou et al., 2001). Although the KcsA channel contains only two transmembrane segments and is found in a prokaryotic cell, it has been adopted as a model system for the general mechanism by which ion channels achieve rapid permeation accompanied by strong ion selectivity. Recent data on the structure of KvAT that has six transmembrane helices (as do the majority of voltage-dependent K$^+$ channels) indicated that the selectivity filter is essentially identical to that of KcsA (Jiang et al., 2003).

Diverse ion species have been used to study gating and permeation mechanisms; it has been shown that for K$^+$ channels, both K$^+$ and Rb$^+$ are both highly permeable. The presence of permeant cations in the external solution slow the closing of K$^+$ channels, while

---

Address correspondence to Heinrich Terlau, Max-Planck-Institute for Experimental Medicine, Molecular and Cellular Neuropharmacology Group, Hermann-Rein-Str.3, D-37075 Göttingen, Germany. Fax: 49-551-3899-475. email: hterlau@gwdg.de

A. Boccaccio's present address is International School for Advanced Studies, S.I.S.S.A., Sector of Neurobiology, Via Beirut 2, 34014 Trieste, Italy.

activation kinetics are relatively unaffected (Swenson and Armstrong, 1981; Matteson and Swenson, 1986). The experiments with different ion species suggest that gating and permeation of K^+ channels are not totally uncoupled, and that the cations in the pore affect channel gating, particularly deactivation and inactivation rates. It has been hypothesized that Rb^+, which enters the channel as well as K^+, binds more tightly and therefore has a larger effect on the closing rate than the more loosely bound K^+. In addition, the rate of C-type inactivation is affected by occupancy at a binding site near the external mouth of the pore (López-Barneo et al., 1993).

Surprisingly, the distribution of Rb^+ and K^+ in the selectivity filter differs even though both ions are highly permeable (Morais-Cabral et al., 2001). The structures of MacKinnon and coworkers reveal that Rb^+ strongly prefers sites 1 and 3 (starting from the outer side of the selectivity filter) (Morais-Cabral et al., 2001) over a site 2 and 4 occupancy configuration. In this study, we used a specific toxin to investigate K^+ channels; as the close interaction of toxins with channel proteins can be sensitive to ion occupancy and, in principle, provide information about the dynamic activity of the channel during gating. κ-Conotoxin PVIIA (κ-PVIIA), isolated from the fish-hunting *Conus* species *C. purpurascens*, selectively blocks the voltage-gated *Shaker* K^+ channel (Terlau et al., 1996) and binds in a bimolecular fashion to the extracellular mouth of the pore (Shon et al., 1998). The peptide interacts strongly with amino acid residues known to be at the outer pore vestibule (Terlau et al., 1996; Shon et al., 1998; Jacobsen et al., 2000).

κ-PVIIA shares common features with the scorpion toxin charybdotoxin (CTX) in its binding to K^+ channels, such as dependence of block on the ionic composition of the medium (for CTX, Anderson et al., 1988; MacKinnon and Miller, 1988; Goldstein et al., 1994; for κ-PVIIA, Scanlon et al., 1997; Garcia et al., 1999; Terlau et al., 1999). The previous analysis of κ-PVIIA block of the *Shaker* channel demonstrated a state dependence: the potency of toxin block in the open conformation decreased with increasing potential; the off-rate was strongly voltage dependent while the on-rate was voltage insensitive. This voltage dependence was explained by interaction with K^+ in the pore, first proposed for CTX block of large-conductance Ca^{2+}-activated K^+ channels (BK) and *Shaker* channels (MacKinnon and Miller, 1988; Goldstein and Miller, 1993). When K^+ is the only permeant ion present, open channel block is not affected by the extracellular K^+ concentration, $[K^+]_o$, and complete removal of intracellular K^+ is necessary to relieve the voltage dependence of the block (Garcia et al. 1999). In contrast, block of the closed state by the toxin is not voltage dependent and decreases upon increasing $[K^+]_o$, a result consistent with competition between κ-PVIIA and K^+ for a binding site at the outer end of the pore (Terlau et al. 1999).

Thus, when toxin binds, it has a strong interaction with ions in the pore. In this study, we show that κ-PVIIA binding to *Shaker* channels in the presence of K^+ and Rb^+ exhibits properties that can be rationalized by differences in the selectivity filter occupancy of these two ions, validating the structural data also in 6TM potassium channels. It is demonstrated that the interaction of κ-PVIIA with the *Shaker* channel in the closed and open conformation is different in the presence of two permeant cations, K^+ and Rb^+. When K^+ is partially or completely replaced by Rb^+, the kinetics and voltage dependence of open-channel block depend on both intracellular and extracellular ionic composition. Thus, the results reveal that κ-PVIIA is sensitive to both differences in the occupancy of the channel pore as well as which specific ion is present in the pore. These data indicate that the ion(s) in the pore functionally affects the receptor site for the toxin.

MATERIALS AND METHODS

Toxin Preparation

The solid-phase peptide synthesis of κ-PVIIA was performed as described in Shon et al. (1998). cRNA for *Shaker*-Δ6-46 (Hoshi et al. 1990) was obtained by a standard protocol (Krieg and Melton, 1987) using a template with a T7 promoter.

Oocyte Expression System

Oocytes from *Xenopus laevis* were prepared as described previously (Stühmer, 1992). RNA was injected into stage V–VI oocytes, and currents were recorded 1–7 d after injection after mechanical removal of the vitelline membrane. For outside-out patch-clamp recordings (Hamill et al., 1981), the aluminum silicate glass pipettes had resistances between 0.8 and 1.2 MΩ. The pipette solution was (in mM) 115 XCl, 1.8 EGTA, 10 HEPES (X indicates either K or Rb). The bath solution contained (in mM) 115 XCl, 1.8 CaCl$_2$, 10 HEPES. The pH was adjusted to 7.2 with TrisBase.

Currents were measured with an EPC-9 patch clamp amplifier driven by the Pulse+PulseFit software package (HEKA Elektronik). Current records were low-pass filtered at 5 kHz and sampled at a rate of 20 kHz.

Leak and capacitive currents were corrected on-line by using a P/n method. Toxin solution was added to the bath chamber by using a Gilson tip pipette. The indicated toxin concentrations correspond to the final concentration in the bath chamber.

Off-line analysis was performed with a Macintosh G3 microcomputer (Apple Computer, Inc.) with self-written programs in the Igor (Wavemetrics) environment.

Kinetic Analysis

To interpret the experimental data, we used a simple bimolecular reaction scheme to describe the interaction between the toxin and the channel, represented by

$$\{U\} \underset{k_{off}}{\overset{k_{on} * [T]}{\rightleftharpoons}} \{B\}$$
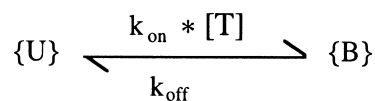
SCHEME I

where {U} represents the toxin-free channels and {B} the channels bound to a toxin molecule; k_{on} is the second order associa-
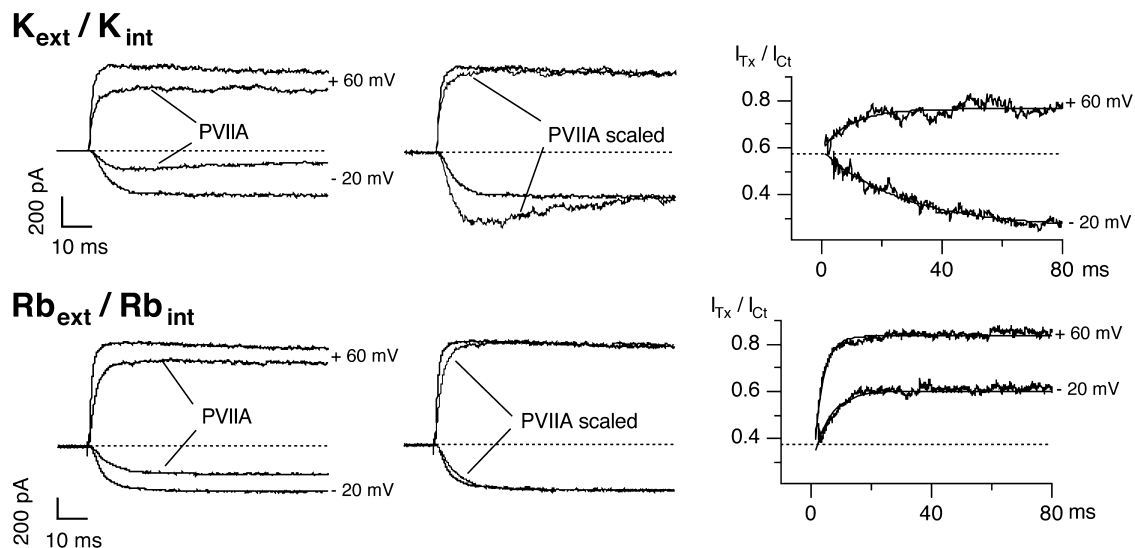
FIGURE 1. κ-PVIIA blocks *Shaker* currents differently in symmetrical K$^+$ and Rb$^+$. (Left) Current responses to voltage steps from a holding potential of −100 mV to −20 and +60 mV, under control conditions and with 200 nM κ-PVIIA in symmetrical K$^+$ (top) and 500 nM κ-PVIIA in symmetrical Rb$^+$ (bottom). (Middle) Current in toxin is scaled to the control to evidence the effect of the toxin. Note that besides a reduction in the current amplitude, also a modification in the kinetics of the current is observed. (Right) Ratio between the toxin and control current traces. The dotted lines correspond to the tonic unblock for closed state, respectively 0.58 in K$^+$ and 0.37 in Rb$^+$, corresponding to a K^C of 265 nM and 293 nM, respectively. The single exponential fits are superimposed to the traces: in symmetrical K$^+$ (top) at +60 mV, τ = 9.56 ms and U = 0.76; at −20 mV, τ = 27.2 ms and U = 0.26. In symmetrical Rb$^+$ (bottom) at +60 mV, τ = 4.6 ms and U = 0.87; at −20 mV, τ = 5.65 ms and U = 0.60.

tion rate constant, [T] is the toxin concentration, and k_{off} is the first order dissociation rate constant (Terlau et al.,1999). Following a step depolarization that opens the channels, U(t) is expected to follow a single-exponential relaxation with time constant τ and asymptotic value U, whose values are related to the open-channel kinetic parameters K^O, k_{off}^O, and k_{on}^O.

From the experimental parameters τ and U, it is possible to evaluate K^O, k_{off}^O, and k_{on}^O according to the inverse relationships:

$$K^O = \frac{[T] \cdot U}{1 - U};$$ (1)

$$k_{off}^{\ O} = \frac{U}{\tau};$$ (2)

$$k_{on}^{\ O} = \frac{1 - U}{[T] \cdot \tau}.$$ (3)

For the open channels, the unblock probability U(t) is calculated at any potential step from the ratio between the current in the presence of toxin and under control conditions (Figs. 1 and 2). The kinetics of κ-PVIIA binding to the closed channels was evaluated with a double pulse protocol, where each stimulus consisted of two identical pulses (at −20 or −30 mV for symmetric K$^+$, at −30 or +40 mV for symmetric Rb$^+$) separated by a time interval, Ti, at the holding potential (between –80 and −100 mV), increasing from 5 ms to 5 s. With such a protocol, one measures the time course of the re-equilibration of the binding to closed channels after the perturbance produced by the first pulse (Terlau et al., 1999).

RESULTS

κ-PVIIA Block in Symmetrical Solutions

The top left panel in Fig. 1 shows the responses to depolarizing pulses (V$_H$ = −100 mV, V$_P$ = +60 and −20

mV) for a representative outside-out patch experiment exposed to symmetric 115 mM K$^+$ solutions, before and after the addition to the external bath of 200 nM κ-PVIIA. At this concentration, κ-PVIIA blocks ∼75% of the steady-state inward current at −20 mV with an apparent dissociation constant, K^O, of ∼67 nM, but has a smaller effect on the currents at larger depolarizations, the block being ∼25% at +60 mV, corresponding to a nine times larger K^O of ∼600 nM. The time course of the currents in presence of the toxin is modified: at both voltages, the early currents are reduced by ∼40%, however, the inward currents show a late inactivation-like decrease ("hump"), whereas the outward currents show a slower additional increase after activation of control currents is maximal. This is shown more clearly in the top middle panel where the traces in the presence of κ-PVIIA are scaled to have the same steady-state level as the control traces. The hump is observed because at this test potential, the affinity of the toxin to the open channels is higher than to the closed channels, and the kinetics of toxin relaxation is slower than the activation kinetics (Terlau et al., 1999). The ratio of toxin to control traces can be taken as representative of the unblocked channels, i.e., the unblock probability; as illustrated in the top right panels, depolarizations to −20 mV produce an increase in the block during the pulse, while for the depolarization to +60 mV, an unblock is observed. The ratios are well fitted by a single exponential (continuous lines) with time constants de-
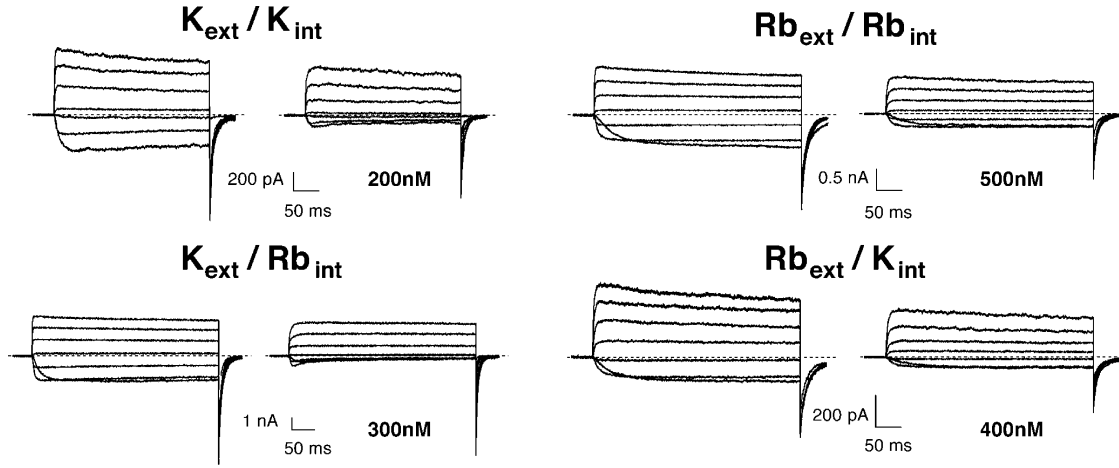
FIGURE 2. κ-PVIIA block of *Shaker* currents in symmetric and asymmetric ionic Rb⁺ or K⁺ solutions. Current records in response to IV protocols ($V_H = -100$ mV, V_P from -50 mV to $+70$ mV, every 20 mV) recorded with outside-out patch clamp experiments in symmetrical 115 mM KCl (top left), symmetrical 115 mM RbCl (top right), K_{ext}/Rb_{int} (bottom left), and Rb_{ext}/K_{int} (bottom right) before and after the addition to the bath of κ-PVIIA (concentration indicated in the figure). The reversal potential is $+5$ mV in symmetrical 115 mM KCl, $+3$ mV in symmetrical 115 mM RbCl, $+4$ mV in K_{ext}/Rb_{int}, and -5 mV in Rb_{ext}/K_{int}.

creasing with the applied potential (τ^O is 27 ms at -20 mV and 9.6 ms at $+60$ mV). Together with the asymptotic values of the ratios, interpreted as equilibrium toxin-free probabilities, U^O, these time constants provide estimates of the open-channel dissociation constant, K^O, the second order association rate constant, k_{on}^O, and the first order dissociation rate constant, k_{off}^O, according to Eqs. 1–3. From the data of Fig. 1, we evaluate k_{off}^O to be 9 s⁻¹ at -20 mV and 80 s⁻¹ at $+60$ mV, and k_{on}^O to be 133 s⁻¹μM⁻¹ at both voltages. As previously described (Garcia et al., 1999; Terlau et al., 1999), we find that both K^O and k_{off}^O increase exponentially with voltage, whereas k_{on}^O is fairly voltage inde-

pendent (Table I), i.e., the exponentially decreasing efficiency of κ-PVIIA in blocking open channels is almost exclusively due to the increase in the toxin dissociation rate.

The top right panel of Fig. 1 shows that initial ratio of toxin to control responses is ~0.56 for both -20 mV or $+60$ mV pulses. Interpreting this value as the toxin-free probability at the onset of the voltage step yields an estimate of ~254 nM for the dissociation constant, K^C, for toxin binding to closed channels. In the same experiment, from a double (-20 mV) pulse protocol, we evaluated the recovery of tonic κ-PVIIA binding to closed channels with a time constant, τ^C, of 720 ms (unpub-

T A B L E I

Dependence of κ-PVIIA Binding Parameters to Shaker-Δ Channels on the Solution Composition

		Open channel block				Closed channel block		
Extra	Intra	$K^O(0)$	v_s	k_{on}^O	$k_{off}^O(0)$	K^C	k_{on}^C	k_{off}^C
		nM	*mV*	*μM⁻¹s⁻¹*	*s⁻¹*	*nM*	*μM⁻¹s⁻¹*	*s⁻¹*
K⁺	K⁺	148 ± 52	41 ± 6	155 ± 61	21 ± 9	246 ± 69	1.9 ± 0.5 (*)	0.6 ± 0.3 (*)
Rb⁺	Rb⁺	1023 ± 192	76 ± 10 (1.7 ± 0.3%) mV⁻¹	119 ± 58	150 ± 26	241 ± 41	>>25 (**)	>>5 (**)
K⁺	Rb⁺	252 ± 21	32 ± 3	94 ± 48 ($V_P < 0$)	18 ± 6	308 ± 35	2.7 ± 0.6	0.9 ± 0.1
Rb⁺	K⁺	231 ± 50 ($V_P > 0$)	45 ± 6 ($V_P > 0$)	104 ± 20 ($V_P > 0$)	30 ± 10 ($V_P > 0$)	139 ± 31		

Patch-clamp experiments performed in the outside-out configuration, number of experiments between 4 and 14, with 1–4 toxin applications for each experiment. The toxin concentrations used varied between 100 nM and 1 μM (K_{ext}/K_{int}: 100–400 nM; K_{ext}/Rb_{int}: 100–400 nM; Rb_{ext}/K_{int}: 100–500nM; Rb_{ext}/Rb_{int}: 300–1,000 nM). Open channel block parameters were pooled from data collected at V_P between -60 and $+80$ mV, if not otherwise stated. $K^O(0)$ and v_s are the mean values of the single exponential fit parameters obtained for each experiment. In symmetrical Rb, the weaker voltage dependence can also be described with a linear fit. Mean values (±SD) are reported, otherwise obtained (*) from fit of the τ as a function of [T] with $\tau = 1/(k_{off} + k_{on}^*$ [T]). For the symmetrical Rb case (**) a lower limit estimate is obtained from $k_{off} = (1/\tau)^* (K^C/(K^C + [T]))$; $k_{on} = (1/\tau)/(K^C + [T])$ when $\tau \gg \tau_d$, where τ_d is the channel deactivation time.
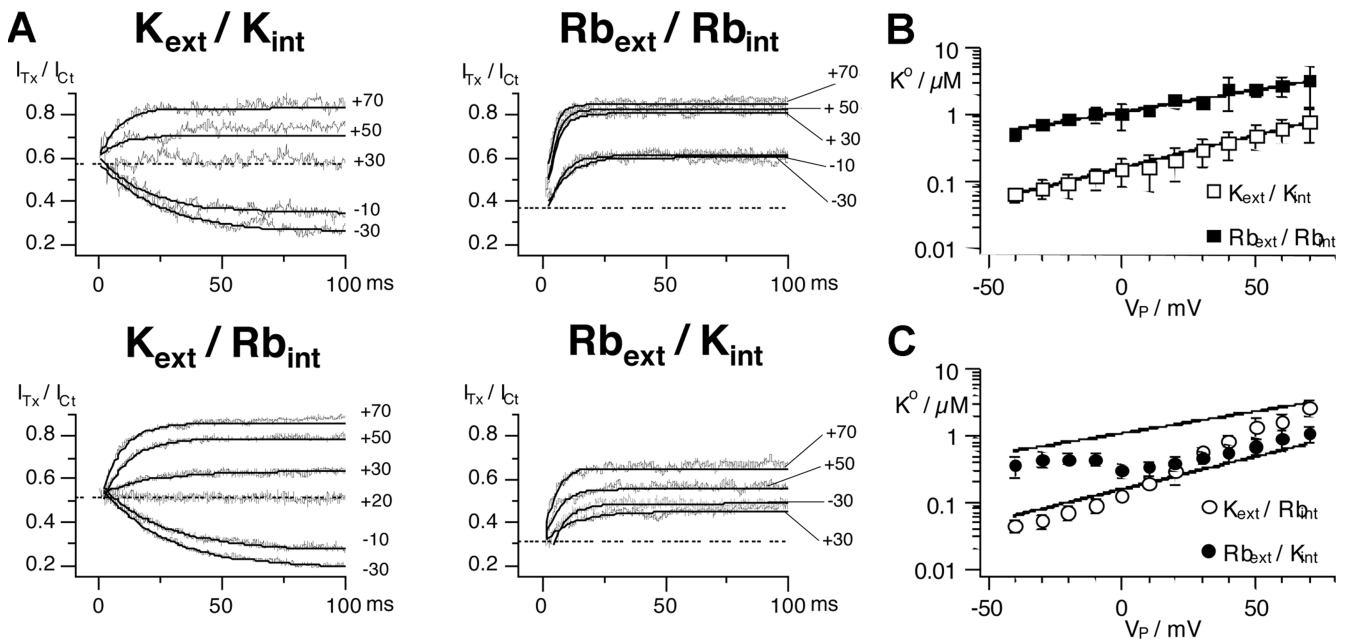
FIGURE 3. Relaxation of κ-PVIIA block of *Shaker* currents depends on the permeant cation, Rb^+ or K^+. (A) Ratios between toxin and control current traces from the IV experiments in Fig. 2 from IV protocols ($V_H = -100$ mV, V_P from -50 mV to $+70$ mV, every 20 mV) in different ionic conditions (symmetrical K^+ with 200 nM κ-PVIIA, symmetrical Rb^+ with 500 nM, K_{ext}/Rb_{int} with 300 nM, and Rb_{ext}/K_{int} with 400 nM). (B) Semilogarithmic plot of the mean values $\pm$ SD of the dissociation constants (K^O) versus test potential for symmetrical K^+ (empty squares) or symmetrical Rb^+ (filled squares). The continuous lines correspond to the exponential fit with $K^O(V) = K^O(0)*\exp(-V/vs)$, with $K^O = 146$ nM at 0 mV and vs = 43 mV for symmetrical K^+ and 1023 nM and vs = 76 mV for symmetrical Rb^+. (C) K^O versus Vp for K_{ext}/Rb_{int} and Rb_{ext}/K_{int} together with the fits from B.

lished data). This yielded the following estimates: $k_{off}^C = 0.78$ s^{-1} and $k_{on}^C = 3.1$ μM^{-1}s^{-1} (see Table I for mean values).

When similar experiments are performed in the presence of symmetrical 115 mM RbCl (Fig. 1, bottom), the most obvious difference is that the κ-PVIIA block of open channels is much weaker and much less voltage dependent, although the initial values of toxin to control currents (Fig. 1, bottom right) indicate a toxin binding affinity to closed channels similar to that observed in symmetric K^+ conditions ($K^C \sim 270$ nM). As a consequence, channel opening entrains κ-PVIIA unbinding at all activating voltages, and in particular the inward current at -20 mV lacks the hump that in symmetrical K^+ reveals an increase in toxin affinity (compare the scaled traces in the top and bottom middle panels of Fig. 1). In the experiment of Fig. 1, 500 nM κ-PVIIA blocked only $\sim$38% of the steady-state inward current at -20 mV and $\sim$17% of the outward current at $+60$ mV, with apparent K^O values of 820 nM at -20 mV and three times larger ($\sim$2.4 μM) at $+60$ mV.

We also notice that in symmetrical Rb^+, toxin binding relaxations, as revealed by the ratios of toxin to control currents, have faster kinetics. From the data of Fig. 1 (bottom right), the estimated time constants are 5.65 ms at -20 mV and 4.6 ms at $+60$ mV; together with the K^O values reported above, these time constants yield

k_{off}^O estimates of 109 s^{-1} at -20 mV and 180 s^{-1} at $+60$ mV, and k_{on}^O estimates of 133 s^{-1}μM^{-1} at -20 mV and 74 s^{-1}μM^{-1} at $+60$ mV. Thus, the main effect of replacing K^+ for Rb^+ appears to be an increase of k_{off}^O that makes toxin binding weaker and with faster kinetics; in addition, k_{off}^O is much less voltage dependent and a significant decrease of k_{on}^O appears to contribute to the increase of K^O with voltage.

The differences observed for κ-PVIIA binding to open and closed channels in the presence of these two cations were unexpected, because Rb^+ is almost as permeable as K^+ and readily enters the pore.

Comparison with κ-PVIIA Block Under Bi-ionic Conditions

To further investigate the very different interaction of κ-PVIIA with the *Shaker* channel depending on the type of ion that occupies the pore, similar experiments were also performed under asymmetric bi-ionic conditions. Fig. 2 shows a comparison of the current recordings obtained from outside-out patches under symmetrical K^+ and Rb^+ conditions with the currents from similar experiments with K_{ext}/Rb_{int} or Rb_{ext}/K_{int} (IV protocols: $V_H = -100$ mV, V_P from -50 mV to $+70$ mV, every 20 mV). As can be seen directly, the inward currents are blocked by κ-PVIIA more than the outward currents measured at high depolarizations under all four conditions. Nevertheless, the hump observed for the inward

currents in the presence of toxin for symmetrical K^+ is only present also for K_{ext}/Rb_{int} but not for the other two conditions. To further compare these data, the unblock probability for the current records from all four conditions were calculated and are shown in Fig. 3.

The top panels of Fig. 3 show the properties of κ-PVIIA block in symmetrical Rb^+ or K^+ conditions shown in Fig. 2, as revealed by the estimated records of the unblock probability, $U(t) = I_{Tx}/I_{ct}$, following pulse potentials in the range of -50 to $+70$ mV, whereas the bottom panels show the same kind of data obtained with K_{ext}/Rb_{int} or Rb_{ext}/K_{int}.

The top left panel of Fig. 3 shows data for symmetrical K^+ and 200 nM κ-PVIIA. It is seen that for depolarizations below $+30$ mV, U decreases during the pulse, while above this potential, an unblock is observed. At about $+30$ mV, the closed channel block appears to be equal to the open channel block, so that the ratio $U(t) = I_{Tx}/I_{ct}$ remains constant during the pulse. The horizontal dotted line shows the estimated unblock probability of the early currents, which is independent of the pulse potential and corresponds to a dissociation constant for κ-PVIIA binding to closed channels, K^C, of ~270 nM (Terlau et al., 1999). Fitting $U(t)$ records with single exponentials (continuous lines) yields time constants that decrease monotonically with voltage from 24 ms at -30 mV to 8 ms at $+70$ mV, and estimates of the asymptotic toxin-free probabilities that increase with voltage from 0.26 at -30 mV to 0.85 at $+70$ mV. Using Eqs. 1–3, we estimate that between -30 and $+70$ mV, K^O increases ~16-fold, from 69 nM to 1.13 µM; k_{on}^O decreases by $\sim60\%$, from 155 to 94 $s^{-1}µM^{-1}$; and k_{off}^O increases ~10-fold, from 11 to 106 s^{-1}, and is the main determinant of the destabilization of toxin binding at increasing depolarizations. At variance with kinetic parameters, steady-state toxin-free probabilities can also be obtained from tail currents, even for voltages near the reversal potential (unpublished data). Thus, K^O estimates are in general more accurate and detailed in the whole voltage range of -50 to $+80$ mV. In the K_{ext}/K_{int} experiment of Fig. 3 A, the voltage dependence of K^O was fitted by a simple exponential, $K^O(V) = K^O(0)*exp(-V/vs)$, with $K^O(0) = 159$ nM and vs = 37 mV. A semilogarithmic plot of mean $K^O(V)$ estimates ($\pm$SD) is given in Fig. 3 B as open squares. The straight line fitting the mean data corresponds to $K^O(0) = 148$ nM and vs = 41 mV (Table I).

Analogous data for symmetrical Rb^+ and 500 nM κ-PVIIA are shown in the top right panel of Fig. 3 A and as open squares in Fig. 3 B. As described in reference to Fig. 1 and 2, we notice a much faster and more extensive unblock at all potentials with a much weaker voltage dependence. When converted into toxin binding parameters through Eqs. 1–3, the time constants and the steady state of the unblock indicate that the re-

placement of K^+ with Rb^+ has little effect on the k_{on}^O rate, which is weakly decreasing with voltage and has a mean value close to that of symmetrical K^+ conditions (Table I). The replacement appears to affect predominantly the k_{off}^O rate, which is increased about 10-fold at low depolarizations. In addition, toxin binding to a Rb^+-filled channel is not so much further destabilized at larger voltages as when K^+ is the charge carrier (Fig. 3 B, filled squares; Table I).

$U(t)$ records for K_{ext}/Rb_{int} conditions in the presence of 300 nM κ-PVIIA are shown in the bottom left panel of Fig. 3 A. It is seen that these data are quite similar to those obtained in symmetrical K^+: the inward currents are blocked much more than the outward currents, and toxin block increases for $V < +20$ mV, whereas an unblock occurs at higher potentials. At $+20$ mV, the open channel block is about the same as the closed channel block and no unblock nor reblock is observed. The most significant difference with the case of symmetrical K^+ is that toxin block gets increasingly weaker at positive voltages so that the apparent K^O approaches the larger values observed in symmetrical Rb^+ (Fig. 3 C, open circles).

The bottom right panel of Fig. 3 A shows $U(t)$ records for Rb_{ext}/K_{int} conditions in the presence of 400 nM κ-PVIIA. It is seen that, similarly to the case of symmetrical Rb^+, channel opening entrains toxin unblock at all voltages. However, the unblock does not increase with voltage as strongly as in Rb_{ext}/Rb_{int} conditions. Indeed, comparing the respective $U(t)$ records shows that κ-PVIIA blocks the outward currents at $+30$ mV more than the inward currents at -30 mV. This behavior results in a clearly nonmonotonic voltage dependence of K^O (Fig. 3 C, filled circles), which suggests a rather sharp transition of toxin binding, from a relatively low Rb^+-like to a much higher K^+-like affinity, near the current reversal potential (-5 mV in this experiment).

Kinetics of κ-PVIIA Binding to Closed Channels

The kinetics of κ-PVIIA binding to closed channels can be measured with a double pulse protocol, in which a conditioning pulse to V_P is followed by an identical pulse, separated by an interpulse interval at holding potential of variable duration Ti. The resting period between successive stimulations was at least 5 s in order to restore "tonic" conditions. With such a protocol we tested the reequilibration of the binding to closed channels at different times after the first pulse. As shown by Terlau et al. (1999), the kinetics of the reequilibration of the binding to closed channels is slowed down by increasing the extracellular K^+ concentration (and decreasing Na^+), due to a reduction of the association rate.

Fig. 4 A shows the current responses to such a protocol in symmetrical 115 mM KCl ($V_P = -20$ mV, Vh =

−100 mV, Ti as indicated in figure). We observe that the conditioning pulse induces an increase of toxin block that appears as a reproducible hump in the first response of each successive double stimulation (Terlau et al., 1999). However, for small T_i values, the second response has a shape similar to control conditions in that no peak is observed (in figure Ti = 80 ms). This indicates that the fraction of blocked channels is near the equilibrium for open-channel block at −20 mV that was achieved by the end of the conditioning pulse and corresponded to $U^O = 0.23$. A quantitative analysis of the relaxation process is shown in the inset of Fig. 4 A, by plotting, as a function of T_i, early amplitudes of conditioning responses in toxin normalized to the control value. These data are well fitted by a single exponential increase with T_i with a time constant of 0.72 s. Assuming this value as an estimate of τ^C and using the value of $U^C = 0.5$ measured from the early fraction of unblocked currents (unpublished data), we estimate in this experiment $K^C = 200$ nM, $k_{off}^C = 0.69$ s^{-1}, and $k_{on}^C = 3.5$ μM^{-1}s^{-1}. The estimates given in Table I for k_{on}^C and k_{off}^C are obtained considering the linear dependence of τ^{-1} on the toxin concentration, through the relationship $\tau^{-1} = k_{on}^C * [T] + k_{off}^C$ (Terlau et al. 1999). For the symmetrical 115 mM KCl case, they agree with the values obtained by Terlau et al. (1999).

Fig. 4 B shows a similar experimental protocol recorded in symmetrical 115 mM RbCl for the same experiment in Fig. 2 ($V_P = +40$ mV, $V_H = -100$ mV, Ti as indicated in figure). The responses corresponding to Ti = 10, 34, 66, and 130 ms are superimposed. Clearly the toxin equilibrates very fast with the closed state and 34 ms is enough to reach the equilibrium in 500 nM κ-PVIIA. During the repolarization at V_H, three processes take place: first, since the toxin potency in blocking open channels is higher at more negative potentials, the toxin has to reequilibrate with the open channels at the new potential; second, deactivation occurs; third, the toxin equilibrates with the fraction of channels that are in the closed state. In high extracellular K$^+$, the last process has a much slower kinetics and therefore is easy to separate. In high extracellular Rb$^+$, first, the deactivation is slower, and second, the equilibration to the closed states is faster. Therefore all three processes have the same time scale, and consequently a kinetic analysis of the reblock is not possible.

These observations demonstrate that the occupancy of the pore by Rb$^+$ appears to also hasten the kinetics of κ-PVIIA binding to closed channels. In 115 mM external Rb$^+$, the rebinding of κ-PVIIA to closed channels after an unblocking depolarization appears to be about as fast as channel closing, which in high [Rb$^+$]$_o$ has time constants in the order of 10 ms.
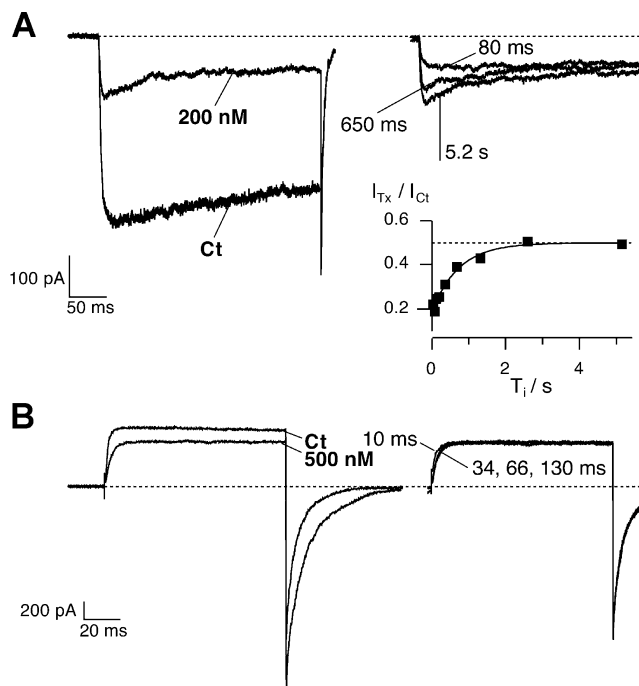

FIGURE 4. Relaxation of κ-PVIIA binding to closed *Shaker-Δ* channels after a depolarizing pulse. Outside-out patch clamp experiments performed in symmetrical 115 mM KCl (A) or 115 mM RbCl (B; same experiment as in Fig. 2). Superimposed records of responses to double pulse stimulation before and after the addition to the bath respectively of 200 nM and 500 nM κ-PVIIA. Each stimulation consisted of a conditioning pulse to V_P, followed with a variable pulse interval, T_i, by an identical test pulse: (A) duration conditioning pulse = 300 ms, $V_P = -20$ mV, $V_H = -100$ mV, T_i shown 80 and 680 ms, and 5.2 s; (B) duration conditioning pulse = 100 ms, $V_P = +40$ mV, $V_H = -100$ mV, T_i shown 10, 34, 66, and 130 ms. (A) Symmetrical 115 mM KCl. The conditioning pulse induces an increase of toxin block that appears as a hump in the first response; in the second response for small T_i values no peak is observed. (A, inset) Amplitude of the second response at early time normalized to the control response and plotted as a function of T_i. The continuous line is the best exponential fit with $\tau = 720$ ms, and the dotted horizontal line corresponds to the asymptotic value of $U = I_{Tx}/I_{Ct} = 0.50$, giving $K^C = 200$ nM. From U and τ from Eqs. 2 and 3, we estimate $k_{off}^C = 0.69$ s^{-1} and $k_{on}^C = 3.5$ μM^{-1}s^{-1}. (B) Symmetrical 115 mM RbCl. The toxin equilibrates very fast with the closed state and 60 ms is enough to reach the equilibrium: the responses to the second pulse are indistinguishable after 66 ms. The process of toxin equilibration with the fraction of channels that are in the closed state has the same time scale of the deactivation process. Consequently, a kinetic analysis of the reblock is not possible.

DISCUSSION

The recent crystallographic data revealed differences between K$^+$ and Rb$^+$ in occupancy of binding sites in the narrow selectivity filter of KcsA (Morais-Cabral et al., 2001). Although the prokaryotic KcsA channel contains only two transmembrane segments, its pore structure provides a solid basis for understanding how potassium channels achieve large and strongly selective per-

meation, and recent data on the structure of KvAT (that has six transmembrane helices as *Shaker*) indicate that the selectivity filter is essentially identical to that of KcsA (Jiang et al. 2003). Accordingly, different preferences of K^+ and Rb^+ for the occupancy of binding sites within the pore of the *Shaker* channel may explain many features of the results with κ-PVIIA binding documented in this study.

It has been proposed that the interaction with K^+ ions in the permeation pathway is the major determinant of the properties of κ-PVIIA binding (Garcia et al., 1999; Terlau et al., 1999). Permeant ions penetrating the ion pore from the intracellular side destabilize an extracellularly bound toxin with a probability that increases with voltage. If the channel pore affords a single-file multiple ion occupancy, the destabilizing configuration likely results from the concerted movement of two or three ions, each traversing only a fraction of the electrical distance across the pore. The above mechanism has been supported by recent structural work demonstrating that K^+ channels are indeed multi-ion pores (Doyle et al., 1998; Morais-Cabral et al., 2001; Zhou et al., 2001). With K^+ as the only permeant ion present, the "on" binding of κ-PVIIA to the extracellular vestibule of an open channel may be little sensitive to $[K]_o$ and to voltage because any hindering ion at the outer pore entrance could easily be pushed inwardly by the incoming toxin, whereas the occupancy configuration of the ion sites within the pore is expected to have a strong effect on the toxin "off" rate and to be strongly voltage dependent (Terlau et al., 1999). When Rb^+ solutions are used on both sides of the membrane, the control current does not differ from traces recorded in symmetrical K^+, indicating normal permeation for Rb^+ through the *Shaker* channel. Under these conditions, the pore is loaded exclusively with Rb^+, and when the toxin is applied, block potency is strongly reduced and the voltage dependence is much less steep (Figs. 1–3). Rb^+ and K^+ have similar radii and both readily enter the channel, as shown also by the fact that in bi-ionic conditions the current reversal potential is close to zero.

In the cartoons of Fig. 5, the numbers 1–4 indicate the four sites that a permeant ion encounters within the selectivity filter while moving inward through the narrow region of the pore, and S0 indicates the external ion-binding site. For simplicity, only the most likely populated ion occupancy configurations revealed by the structural study of Morais-Cabral et al. (2001) are taken into account. At high concentrations of permeant ions, as occurring in the experimental conditions explored in this work, these configurations involve the occupancy of the inner pore sites by two ions. When the channel is closed, the occupancy of S0 plays a major role for toxin binding and is solely determined

by the species and concentration of permeant ions in the extracellular solution. At high $[K]_o$, the probability of S0 occupancy is very high, also because it is compatible with two more ions occupying positions 2 and 4, a configuration that is equally favored by potassium ions as the 1,3 alternative. The mutant cycle analysis data on the binding of κ-PVIIA with *Shaker* (Jacobsen et al., 2000) suggests that the toxin interacts intimately with the pore and an interaction of the toxin with an external ion (one of the external binding sites in Bernèche and Roux, 2001, and Zhou et al., 2001; here called S0) is very likely (see also Moran, 2001). Therefore, κ-PVIIA will compete with K^+ for this site, and toxin binding to the channel will occur only for the configurations in which S0 is not occupied and the inner ions are in the 1,3 position, so that the "on" binding rate is strongly reduced at high $[K]_o$. However, after κ-PVIIA binding, the inner ions can easily shift to the 2,4 configuration, consolidating the binding.

The preference of Rb^+ for sites 1 and 3 revealed by the x-ray data for KcsA provides an explanation for the very different binding kinetics observed in high $[Rb]_o$ on the basis of two considerations: (1) the probability that S0 is occupied by an ion is much lower in Rb, because it cannot be favored by the 2,4 configuration of the inner ions, and this makes the "on" binding rate much larger; (2) upon toxin binding, the shift to the 2/4 configuration which occurs with K^+ is not favored in Rb^+, resulting in a faster unblock. Upon channel opening, two major factors modify toxin binding. On one hand, the occupancy of site S0 is in no case an absolute obstacle for the "on" binding, because the ion in S0 has a relatively free way to escape the toxin repulsion by moving to inner positions. If, while moving along the binding-reaction pathway, the toxin does not feel the ion repulsion before reaching the peak of the free-energy barrier, then we expect a k_{on} rate that is fairly independent of solution composition, as observed.

Quite different considerations apply for the rate of toxin dissociation, which depends on the interaction of the bound toxin with the ions inside the pore and is expected to be quite different for different site-occupancy configurations. For potentials that drive inward currents, the relatively high affinity of κ-PVIIA when K^+ is the charge carrier can be explained by assuming κ-PVIIA binding can push K^+ into the 2/4 configuration in the open state, which leads to the observed increase in affinity measured as a hump in the currents. For outward currents, κ-PVIIA most likely is pushed away by the permeant K^+ (Fig. 5).

For Rb^+ as charge carrier, unblock after opening of the channel was always observed (Fig. 5). The 1/3 preference of Rb^+ for the closed state results in a low occupancy of S0; activation would lead to an increase in occupancy of this site, resulting in the observed unblock
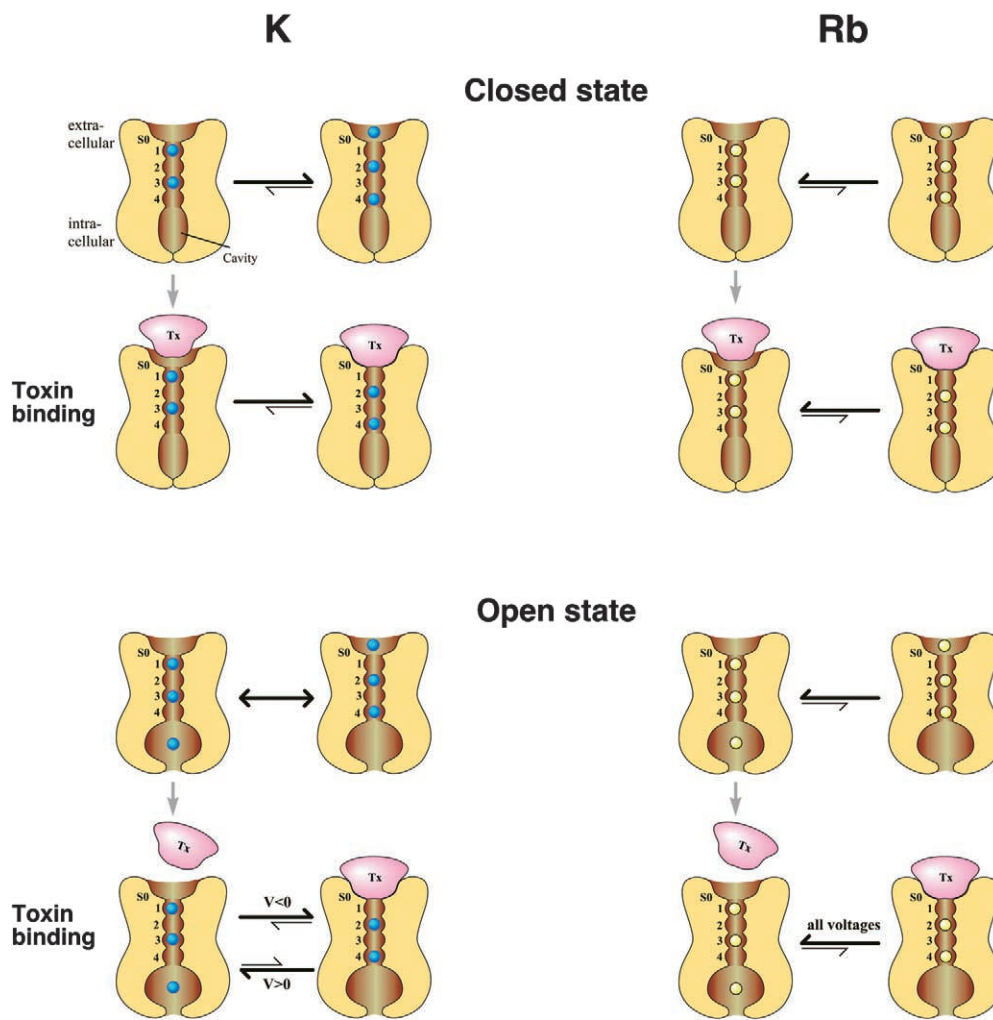
FIGURE 5. Cartoon of κ-PVIIA binding to *Shaker* K$^+$ channels in the presence of Rb$^+$ or K$^+$. κ-PVIIA binding interacts differently with the ion(s)–channel complex depending on the state of the channel (top panel, closed state; bottom panel, open state) and on the pore occupancy of the permeant ion species (left panel, K$^+$; right panel, Rb$^+$). Ion binding sites within the selectivity filter are numbered from 1 to 4, while S0 is the extracellular binding site for K$^+$. A detailed description is given in the Discussion.

at all voltages. Interestingly, with Rb$^+$ as a charge carrier, the block of κ-PVIIA is much less voltage dependent, and fast binding/unbinding kinetics are observed with both inward and outward currents. These data indicate that the 1/3 preference of Rb$^+$ leads to destabilization of toxin binding to the open state, and that in the Rb$^+$-occupied channel pore, the binding site for κ-PVIIA has a different character (either due to slight conformational changes or because the ensemble of accessible states has a different distribution of charge) than for K$^+$, resulting in a different interaction with the toxin. Thus, κ-PVIIA binding to *Shaker* channels is sensitive not only to differences in ion occupancy within the pore but also to subtle differences in the channel-permeant ion complex.

Interestingly, the recent results of Thompson and Begenisish (2003) suggest that the effects of extracellular tetraethylammonium (TEA) on K$^+$ channels are also affected differentially by K$^+$ and Rb$^+$, although the observed effects are somewhat smaller in magnitude than those documented above. The ion replacement studies showed that the identity of the permeant ion in the in-

ternal solution determined the slight voltage dependence of extracellular TEA block, believed to be due to the fact that the TEA binding site is within the membrane electric field. Voltage dependence of TEA block in K$^+$ solutions arises through the movement of K$^+$ ions through some part of the membrane electric field; this voltage dependence was lost with Rb$^+$ as the permeant ion.

Previously, the same authors reported evidence for different patterns of occupancy of specific sites in the pore by permeant ions; K$^+$ and Rb$^+$ interfered differently with the blocking ability of intracellular and extracellularly applied TEA. In *Shaker* channels, external TEA antagonizes the effectiveness of internal TEA only when K$^+$ ions are in the intracellular and extracellular solution (Thompson and Begenisish, 2000). On the contrary, when Rb$^+$ is the permeant ion, external TEA is entirely ineffective in protecting the channels from block by internal TEA, even if external TEA binds slightly more efficiently in the presence of Rb$^+$ in the extracellular solution than of K$^+$. The ability of K$^+$ and the inability of Rb$^+$ to relay interaction between external and in-

ternal TEA seems fully consistent with the freedom of K^+ ions, but not Rb^+, to shift easily in either direction their position inside the narrow region of the pore.

Our data suggest also that having a bound toxin modifies channel gating. This conclusion must be drawn from the fact that closed or open channels have different toxin binding affinity at the equilibrium potential (0 mV and symmetric K^+ or Rb^+). The difference appears to be small in symmetrical K^+ conditions, where closed and open channels have the same toxin affinity for potentials between 20 and 30 mV, but much larger and in the opposite direction in symmetrical Rb^+. Due to obvious considerations of microscopic reversibility at equilibrium, these data imply that the binding of κ-PVIIA slightly favors channel opening if the pore is filled with K^+, whereas it strongly opposes it if the pore is filled with Rb^+. Along the view of interpreting toxin effects as a reflection of the toxin interaction with ions in the pore, this suggests in turn that the channel gating structures depend on ion occupancy. Recent structural data provided evidence that the pore is not rigid, but on the contrary, a dynamic structure (Perozo et al., 1999; Liu et al., 2001; Zhou et al., 2001). Minor adjustments in the structure of the selectivity filter may occur in the different occupational states and with different ion species. By using electron paramagnetic resonance spectroscopy on the KcsA channel, Perozo et al. (1998, 1999; Liu et al. 2001) showed that during gating, significant conformational changes take place near the intracellular end, producing a large increase in the diameter of the vestibule below the central water-filled cavity while the outer vestibule is not greatly affected by the transitions between open and closed state, (Perozo et al., 1999; Liu et al., 2001). However, a small increase in the diameter of the permeation pathway was observed (Liu et al., 2001), supporting the possibility of a dynamic role of the selectivity filter in contributing to the gating mechanism. Structural data (Zhou et al., 2001) showing that the selectivity filter has two significantly different structures, a nonconductive state in low $[K^+]$ and a conductive one in high $[K^+]$, has been obtained, consistent with some structure adjustments while the ions move along the selectivity filter (Zhou et al., 2001). Our data demonstrate that for the binding of κ-PVIIA to *Shaker* K^+ channels, the toxin sees a different interaction partner depending on both the state of occupancy of the pore and the nature of the permeant ions, and the small movements or conformational changes due to ions in a pore can have significant pharmacological and functional impacts. These specific results with κ-PVIIA and the *Shaker* channel may be more broadly relevant, and suggest that channel pores should not be conceptualized as rigid polypeptide cages, but as dynamic structural complexes that change dependent on the permeant ions present.

REFERENCES

Anderson, C.S., R. MacKinnon, C. Smith, and C. Miller. 1988. Charybdotoxin block of single Ca^{2+}-activated K^+ channels. Effects of channel gating, voltage and ionic strength. *J. Gen. Physiol.* 91:317–333.

Armstrong, C.M. 1971. Interaction of tetraethylammonium ion derivatives with the potassium channels of giant axons. *J. Gen. Physiol.* 58:413–437.

Bernèche, S., and B. Roux. 2001. Energetics of ion conduction through the K^+ channel. *Nature.* 414:73–77.

Doyle, A.D., J.M. Cabral, R.A. Pfuetzner, A. Kuo, J.M. Gulbis, S.L. Cohen, B.T. Chait, and R. MacKinnon. 1998. The structure of the potassium channel: molecular basis of K^+ conduction and selectivity. *Science.* 280:69–77.

Garcia, E., M. Scanlon, and D. Naranjo. 1999. A marine snail neurotoxin shares with scorpion toxins a convergent mechanism of blockade on the pore of voltage-gated K^+-channels. *J. Gen. Physiol.* 114:141–157.

Goldstein, S.A.N., and C. Miller. 1993. Mechanism of charybdotoxin block of a voltage-gated K^+ channel. *Biophys. J.* 65:1613–1619.

Goldstein, S.A.N., D.J. Pheasant, and C. Miller. 1994. The charybdotoxin receptor of a *Shaker* K^+ channel: peptide and channel residues mediating molecular recognition. *Neuron.* 12(N6):1377–1388.

Hamill, O.P., A. Marty, E. Neher, B. Sakmann, and F.J. Sigworth. 1981. Improved patch-clamp techniques for high-resolution current recording from cells and cell-free membrane patches. *Pflugers Arch.* 391:85–100.

Hille, B., and W. Schwarz. 1978. Potassium channels as multi-ion single-file pores. *J. Gen. Physiol.* 72:409–442.

Hodgkin, A.L., and R.D. Keynes. 1955. The potassium permeability of a giant nerve fibre. *J. Physiol.* 128:61–88.

Hoshi, T., W. Zagotta, and R. Aldrich. 1990. Biophysical and molecular mechanisms of *Shaker* potassium channel inactivation. *Science.* 250(533):533–538.

Jacobsen, R.B., E.D. Koch, B. Lange-Malecki, M. Stocker, J. Verhey, R.M. Van Wagoner, A. Vyazovkina, B.M. Olivera, and H. Terlau. 2000. Single amino acid substitutions in κ-conotoxin PVIIA disrupt interaction with the *Shaker* K^+ channel. *J. Biol. Chem.* 275(32):24639–24644.

Jiang, Y., A. Lee, J. Chen, V. Ruta, M. Cadene, B.T. Chait, and R. MacKinnon. 2003. X-ray structure of a voltage-dependent K channel. *Nature.* 423:33–41.

Krieg, P.A., and D.A. Melton. 1987. In-vitro RNA-synthesis with SP6 RNA-polymerase. *Methods Enzymol.* 155:397–441.

Liu, Y., P. Sompornpisut, and E. Perozo. 2001. Structure of the KcsA channel intracellular gate in the open state. *Nat. Struct. Biol.* 10:883–887.

López-Barneo, J., T. Hoshi, S.H. Heinemann, and R.W. Aldrich. 1993. Effects of external cations and mutations in the pore region on C-type inactivation of *Shaker* potassium channels. *Receptors Channels.* 1:61–71.

MacKinnon, R., and C. Miller. 1988. Mechanism of charybdotoxin

block of the high-conductance, Ca^{2+}-activated K$^+$ channel. *J. Gen. Physiol.* 91:335–349.

Matteson, D.R., and R.P.J. Swenson. 1986. External monovalent cations that impede the closing of K$^+$ channels. *J. Gen. Physiol.* 87:795–816.

Morais-Cabral, J.H., Y. Zhou, and R. MacKinnon. 2001. Energetic optimization of ion conduction rate by the K$^+$ selectivity filter. *Nature.* 414:37–42.

Moran, O. 2001. Molecular simulation of the interaction of κ-conotoxin-PVIIA with the *Shaker* potassium channel pore. *Eur. Biophys. J.* 30:528–536.

Perozo, E., D.M. Cortes, and L.G. Cuello. 1998. Three-dimensional architecture and gating mechanism of a K$^+$ channel studied by EPR spectroscopy. *Nat. Struct. Biol.* 5(6):459–469.

Perozo, E., D.M. Cortes, and L.G. Cuello. 1999. Structural rearrangements underlying K$^+$-channel activation gating. *Science.* 285:73–78.

Scanlon, M.J., D. Naranjo, L. Thomas, P.F. Alewood, R.J. Lewis, and D.J. Craik. 1997. Solution structure and proposed binding mechanism of a novel potassium channel toxin κ-conotoxin PVIIA. *Structure.* 5:1585–1597.

Shon, K., M. Stocker, H. Terlau, W. Stühmer, R. Jacobsen, C. Walker, M. Grilley, M. Watkins, D.R. Hillyard, R. Gray, and B.M. Olivera. 1998. κ-Conotoxin PVIIA is a peptide inhibiting the *Shaker* K$^+$ channel. *J. Biol. Chem.* 273:33–38.

Stühmer, W. 1992. Electrophysiological recordings from *Xenopus* oocytes. *Methods Enzymol.* 207:319–339.

Swenson, R.P.J., and C.M. Armstrong. 1981. K$^+$ channels close more slowly in the presence of external K$^+$ and Rb$^+$. *Nature.* 291:427–429.

Terlau, H., K. Shon, M. Grilley, M. Stocker, W. Stühmer, and B.M. Olivera. 1996. Strategy for rapid immobilization of prey by a fish-hunting marine snail. *Nature.* 381:148–151.

Terlau, H., A. Boccaccio, B.M. Olivera, and F. Conti. 1999. The block of *Shaker* K$^+$ channels by κ-conotoxin PVIIA is state dependent. *J. Gen. Physiol.* 114:125–140.

Thompson, J., and T. Begenisish. 2000. Interaction between quaternary ammonium ions in the pore of potassium channels. *J. Gen. Physiol.* 115:769–782.

Thompson, J., and T. Begenisish. 2003. External TEA block of *Shaker* K$^+$ channels is coupled to the movement of K$^+$ ions within the selectivity filter. *J. Gen. Physiol.* 122:239–246.

Zhou, Y., J.H. Morais-Cabral, A. Kaufman, and R. MacKinnon. 2001. Chemistry of ion coordination and hydration revealed by a K$^+$ channel-Fab complex at 2.0 Å resolution. *Nature.* 414:43–48.